Organic Electronics 23 (2015) 70–75

Contents lists available at ScienceDirect

Organic Electronics

journal homepage: www.elsevier.com/locate/orgel

Highly stable and high power efficiency tandem organic light-emitting diodes with transition metal oxide-based charge generation layers

Yongbiao Zhao, Swee Tiam Tan, Hilmi Volkan Demir *, Xiao Wei Sun *

Luminous! Center of Excellence for Semiconductor Lighting and Displays, School of Electrical and Electronic Engineering, Nanyang Technological University, 50 Nanyang Avenue, Singapore 639798, Singapore

ARTICLE INFO

Article history:
Received 25 February 2015
Received in revised form 2 April 2015
Accepted 16 April 2015
Available online 17 April 2015

Keywords:
Tandem OLED
Charge generation layer
Stability
Power efficiency improvement
Transition metal oxide

ABSTRACT

Tandem organic light-emitting diodes (OLEDs) have been studied to improve the long-term stability of OLEDs for 10 years. The key element in a tandem OLEDs is the charge generation layer (CGL), which provides electrons and holes to the adjacent sub-OLED units. Among different types of CGLs, n-doped electron transporting layer (ETL)/transition metal oxide (TMO)/hole transporting layer (HTL) has been intensively studied. Past studies indicate that this kind of CGL can achieve the desired efficiency enhancement, however, its long-term stability was reported not good and sometime even poor than a single OLED. This issue was not well addressed over the past 10 years. Here, for the first time, we found that this is caused by the unwanted diffusion of TMO into the underlying n-doped ETL layer and can be well resolved by introducing an additional diffusion suppressing layer (DSL) between them. Our finding will fully release the potential of TMO-based CGL in tandem OLEDs.

1. Introduction

Organic light-emitting diodes (OLEDs) [1] have attracted much attention over past three decades, owing to their high potential in next generation displays and lighting panels. However, before mass production of OLEDs for the consumer market can start, a long operating lifetime must be ensured. It is shown that the lifetime of an OLED (τ), the time that the brightness of OLED drops to half of the initial brightness (L_0), has a strong dependence on L_0: $\tau = \text{const}/(L_0)^n$, where n is the acceleration factor (e.g., 1.8) [2]. This means higher initial brightness L_0 will result in much shorter device lifetime. The mechanism behind is that, higher luminance needs higher driving current density, which will accelerate the degradation of materials and interfaces in the device. Thus it would be much useful if we can significantly reduce the stress on each light-emitting unit while still achieving a given luminance level.

An elegant way to meet this requirement is to stack a number of OLEDs on top of each other, which is the so called tandem OLEDs technology [3,4]. In a tandem OLED, the interconnecting units between two sub-OLEDs that serve as charge generation layers (CGLs) are required when driving OLED stacks as two-terminal devices. Up to now, several CGL structures have been reported, such as n-doped electron transporting layer (ETL)/p-doped hole transporting layer (HTL) (e.g., Alq_3:Li/NPB:$FeCl_3$) [4], organic p/n junction (e.g., CuPc/F16CuPc [5], Pentacene/C60 [6]) and n-doped ETL/electron acceptor/HTL structure (e.g., BCP:Li/MoO_3/NPB [7], Bphen:Li/HAT-CN/NPB [8]). Among them, the use of transition metal oxides (TMOs), such as WO_3, MoO_3, V_2O_5 and ReO_3, as the electron acceptor in the n-doped ETL/electron acceptor/HTL structure has been intensively studied, due to their low cost, easy synthesis and handling compared to their organic counterpart. The charge generation in this kind of CGL was believed to occur at the TMO/HTL interface, where electrons were transferred from the highest occupied molecular orbital (HOMO) of HTL to the conduction band (CB) or defect states of TMO [9–11]. This electron transfer process is much more favored at the TMO/HTL interface, due to the very low lying CBs and work functions (WFs) of TMOs (e.g., CB of MoO_3, WO_3 and V_2O_5 are 6.7, 6.5, and 6.7 eV, respectively) compared to the HOMOs of most HTLs (5.3–6.0 eV) [12].

Up to now, most of studies on TMO-based CGL are focusing on the charge generation mechanism, such as the electronic structure or energy level alignment [9], the critical thickness requirement for each layer [11], or searching for alternative TMOs with better performance [13], which provide important guidelines for making effective CGLs (e.g., double external quantum efficiency, double driving voltage for tandem OLEDs with two sub-OLEDs compared to single OLED). To achieve the long-term stability of tandem OLEDs, the CGL itself should be stable enough under the electrical

* Corresponding authors.
E-mail addresses: volkan@stanfordalumni.org (H.V. Demir), EXWSun@ntu.edu.sg (X.W. Sun).

http://dx.doi.org/10.1016/j.orgel.2015.04.010
1566-1199/

stressing. However, effective CGLs may not imply good long-term stability. For example, Deng found that, the lifetimes of tandem OLEDs with CGLs of Alq_3:Cs_2CO_3/MoO_3/NPB and Alq_3:CsN_3/MoO_3/NPB are about 40 h and 20 h at initial luminance of 1200 cd/m^2, respectively, which are much shorter than that of single OLED [14]. They suggested that the poor lifetime performance was due to the degradation of the n-doped ETL/MoO_3 interface as a result of Caesium cations migration under electrical stressing. Actually, in 2005, Chen observed similar phenomenon (though with different sub-OLED units) [15]. They found that by insertion of a thin (1 nm) metal layer (e.g., Al, Ag) between Alq_3:Cs_2CO_3 and MoO_3 the lifetime of the tandem OLED can be substantially improved and they ascribed the improvement to a better and robust electron and hole injection from the CGL to the two sub-OLEDs. However, they did not point out why this kind of CGL was robust. Later, in 2012, Diez reported one interesting finding that, by insertion a thin interlayer of CuPc or Al_2O_3 between BCP:Cs_3PO_4 and α-NPD:MoO_3 thus forming a CGL with structure of n-doped ETL/interlayer/p-doped HTL, they can increase the device lifetime by a factor of 3.5 [16]. Though the mechanisms for the two interlayers are different, both of them can maximize the stability of the CGL. They considered that the interlayer is needed to prevent chemical reactions or dopant inter-diffusion at the p/n interface leading to an enhanced stability of the devices. From these examples, we can see that the factor that governs the stability of TMO-based CGL is still quite unclear.

In this paper, we found that the diffusion of TMO into the n-doped ETL during the device fabrication process is the root cause for the poor stability of tandem OLEDs with n-doped ETL/TMO/HTL-based CGL. This is evidenced by the fact that inverted tandem OLED with the same CGL shows much better stability compared to the normal tandem OLED. We also demonstrated that insertion of a thin diffusion suppressing layer (DSL) between the n-doped ETL and TMO can substantially suppress the diffusion of TMO into the underlying n-doped ETL, which in turn improves the stability of the resulting tandem OLEDs. The improvement was found to be closely related to the thermal property of the DSL and the one with best stability showed the best performance. More importantly, the power efficiency of the result tandem OLEDs was greatly improved, which surpassed that of the reference single OLED. This finding will fully open the potential of TMO-based CGLs in tandem OLED applications.

2. Experimental

All devices were fabricated on commercial ITO-coated glass substrates. The ITO substrates were treated in order by ultrasonic bath sonication of detergent, de-ionized water, acetone and isopropanol, each with a 20 min interval. Then the ITO substrates were dried with nitrogen gas and baked in an oven at 80 °C for 30 min. After that, oxygen plasma treatment was carried out in a plasma cleaner (FEMTO). Subsequently, the substrates were transferred into a thermal evaporator, where the organic, inorganic and metal functional layers were grown layer by layer at a base pressure better than 4×10^{-4} Pa. The evaporation rates were monitored with several quartz crystal microbalances located above the crucibles and thermal boats. For organic semiconductors and metal oxides, the typical evaporation rates were about 0.1 nm/s and for aluminum, the evaporation rate was about 1 to 5 nm/s. The intersection of Al and ITO forms a 1 mm × 1 mm active device area. *J–V* and *L–V* data were collected with a source meter (Agilent B2902A) and a calibrated Si-photodetector (Thorlabs, FDS-1010CAL) with a customized Labview program. The lifetime study was done in a nitrogen filled glovebox.

3. Results and discussions

3.1. Recall the problem of non-inverted tandem OLEDs with TMO-based traditional CGL

To recall the problem, let's make a comparison between the normal single OLED and normal tandem OLED based on n-doped ETL/TMO/HTL-type CGL. As shown in Fig. 1a, the structures for the normal single OLED and the normal tandem OLED are ITO/MoO_3(2 nm)/NPB(80 nm)/Alq_3(60 nm)/Cs_2CO_3(1 nm)/Al and ITO/MoO_3(2 nm)/NPB(80 nm)/Alq_3(60 nm)/Bphen:30 wt.% Cs_2CO_3(20 nm)/MoO_3(10 nm)/NPB(80 nm)/Alq_3(60 nm)/Cs_2CO_3(1 nm)/Al(150 nm), respectively, where NPB/Alq_3 is the sub-OLED unit, Bphen:30 wt.% Cs_2CO_3/MoO_3/NPB is the n-doped ETL/TMO/HTL-type CGL. The results are shown in Fig. 1. Compared with the normal single OLED, the normal tandem OLED needs a voltage that is a little more than double of the normal single OLED to achieve the same current density (Fig. 1b), the current efficiency of the normal tandem OLED is more than double of the normal single OLED (Fig. 1c) and the power efficiency of the normal tandem OLED is a little lower than that of the normal single OLED (Fig. 1d). All these indicates the Bphen:Cs_2CO_3/MoO_3/NPB is an effective CGL. However, the long-term stabilities of the two OLEDs are surprisingly quite different. As shown in Fig. 1e, at a constant driving current density of 50 mA/cm^2, the luminance of the normal tandem OLED drops to 70% of its initial luminance within 3 h, where it is about 87% for the normal single OLED. At the same time, as shown in Fig. 1f, the driving voltage of the normal tandem OLED increases rapidly from 20.5 V to more than 25 V, with a increment of more than 20%, where it is marginal for the normal single OLED. These observations are similar to the reports of Chen [15] and Deng [14].

By comparing the structures of the normal single and normal tandem OLEDs, it is obvious that the CGL should be responsible for the poor operational stability of the tandem OLED. Individually, the three components of the CGL, i.e. Bphen:Cs_2CO_3, MoO_3 and NPB, should be stable enough due to the fact that OLEDs with them as ETL [17], hole injection layer [18] or hole transporting layer show good long-term stability. Thus the interfaces in the CGL, Bphen:Cs_2CO_3/MoO_3 and MoO_3/NPB, should be considered further. As the combination of MoO_3/NPB has been applied in OLEDs for a few years and it can greatly improve the stability of the resulted OLEDs [18], the only uncertainty is the Bphen:Cs_2CO_3/MoO_3 interface. As Deng suggested, the Cs cations migration during the electrical stressing of the tandem OLED may be a possible cause for the interface degradation, however, there is no direct evidence for this assumption. And if this is true, similar Cs cations migration process should happen in inverted tandem OLED with the same CGL.

3.2. Performance of inverted tandem OLEDs with TMO-based traditional CGL

To examine this, two inverted OLEDs, termed as inverted single OLED and inverted tandem OLED (as shown in Fig. 2a), with structures of ITO/Al(1 nm)/Cs_2CO_3(1 nm)/Alq_3(80 nm)/NPB(60 nm)/MoO_3(5 nm)/Al(150 nm) and ITO/Al(1 nm)/Cs_2CO_3(1 nm)/Alq_3(80 nm)/NPB(60 nm)/MoO_3(10 nm)/Bphen:30 wt.%Cs_2CO_3(20 nm)/Alq_3-(80 nm)/NPB(60 nm)/MoO_3(5 nm)/Al(150 nm), respectively, are studied. From Fig. 2b–d, we can see that both the driving voltage and current efficiency for the inverted tandem OLED at the same current density are about two times of the inverted reference single OLED and the power efficiency of the two OLEDs are almost the same, which indicates the reverse stack of NPB/MoO_3/Bphen:Cs_2CO_3 CGL can work normally. However, opposite to the case for the normal single and normal tandem OLEDs, as shown in

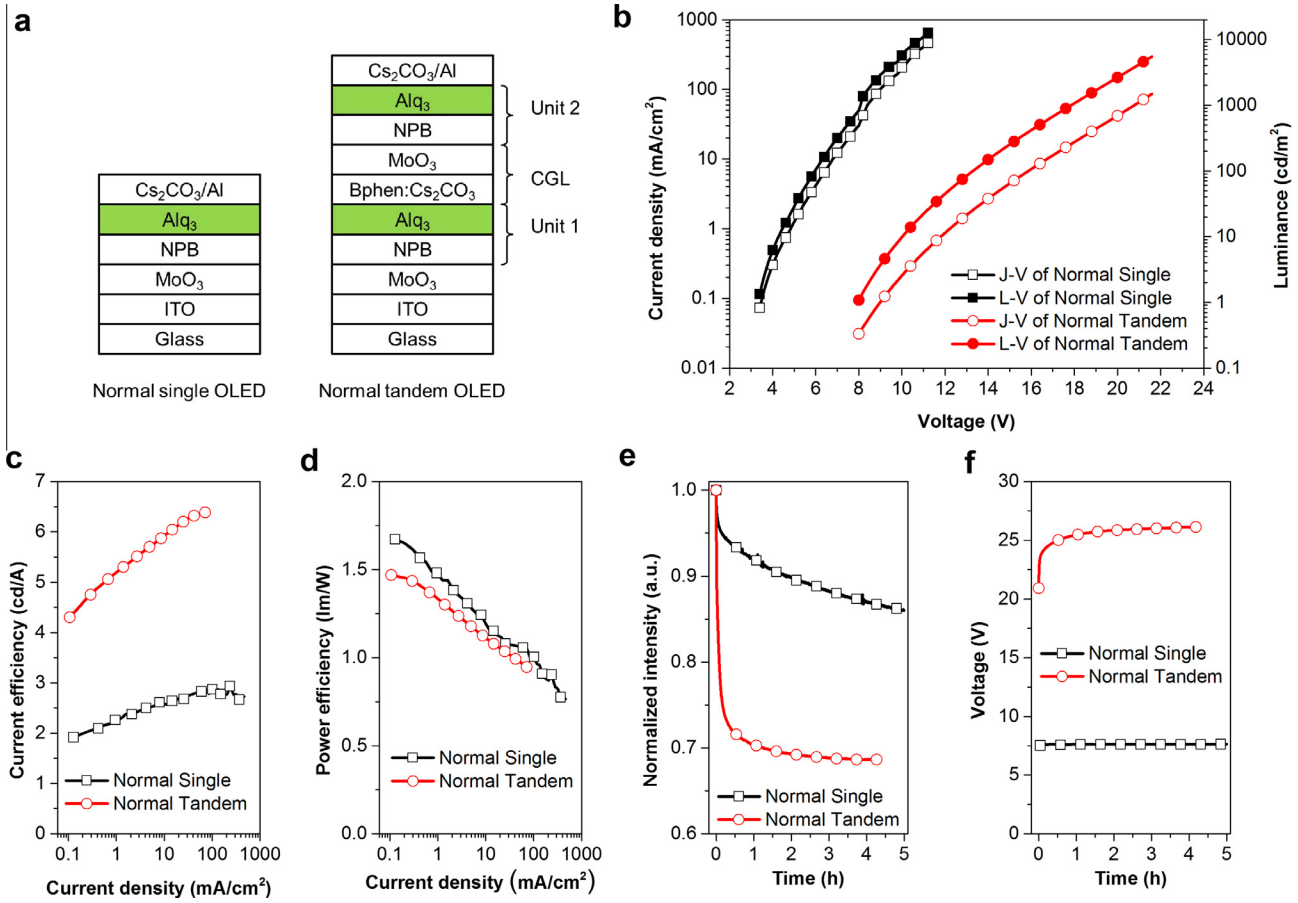

Fig. 1. Device structures and performances of the normal single and normal tandem OLEDs. (a) Device structures for the normal single and normal tandem OLEDs. Both of them are based on NPB/Alq_3 heterojunction. The CGL for the normal tandem OLED is Bphen:30 wt.% Cs_2CO_3 (20 nm)/MoO_3 (10 nm)/NPB. (b) *J–V* and *L–V* curves for the two OLEDs. (c) Current efficiency vs. current density curves and, (d) power efficiency vs. current density curves for the two OLEDs. (e) Luminance and, (f) voltage degradation curves for the normal single and normal tandem OLEDs.

Fig. 2e and f, the long-term stability of the two inverted OLEDs are quite similar. From Fig. 2e it is clear that the luminance degradation processes for the two inverted OLEDs are almost following the same trend. And in Fig. 2f, the voltage degradations for both are marginal. This indicates the degradation mechanism in the normal tandem OLED does not exist or is not so obvious in the inverted tandem OLED. This also means that the proposed Cs cations migration should not be the reason for the degradation in the normal tandem OLED.

3.3. The effect of diffusion suppressing layer on the performance of tandem OLEDs

Based on our previous study [19] that, when TMO is deposited onto organic semiconductor thin film, the TMO will diffuse into the organic thin film and the diffusion depth is depending on the property of the organic semiconductor. For example, depositing MoO_3 onto CBP thin film, the MoO_3 can diffuse more than 20 nm into the CBP layer. We believe this process also happens in tandem OLEDs. As shown in Fig. 3, by comparing the structures of the two tandem OLEDs, it is obvious that in the normal tandem OLED, MoO_3 will diffuse into the Bphen:Cs_2CO_3 layer while in the inverted tandem OLED this will not happen. So we suspect that this difference may cause the different long-term stabilities of the two tandem OLEDs. If this is true, by suppressing the MoO_3 diffusion into the Bphen:Cs_2CO_3 layer, principally, it should be able to improve the long-term stability of the normal tandem OLED. To investigate this, we introduce an additional DSL between the Bphen:Cs_2CO_3 layer and MoO_3 layer in the normal tandem OLED. The device structure for the normal tandem OLED with DSL is shown in Fig. 4a. Firstly, a moderate thickness of 5 nm was chosen for the DSL (shown in Fig. S1). We have employed four organic semiconductors for the DSL for comparison: NPB, Alq_3, Bphen and C60. These four materials have different energy levels and thermal properties. As shown in Fig. 4b and c, compared with the normal tandem OLED without DSL, all the four tandem OLEDs with DSL show reduced driving voltage. A close-up look of Fig. 4c is shown in Fig. 4d. As can be seen, the turn-on voltages are about 5.4, 6.3, 7.0 and 7.1 V for the C60-, NPB-, Alq_3- and Bphen-based tandem OLEDs, respectively, which are much lower than the 8.0 V for the tandem OLED without DSL. For C60 and NPB based devices, the turn-on voltages are even lower than two times of the normal single OLED. This indicates the DSL can effectively reduce the voltage loss across the CGL. From Fig. 4e, it can be seen that there is a marginal increase in the current efficiency with the addition of DSL. The reduced driving voltage and marginal current efficiency improvement indicate that the power efficiency will be enhanced as well. As shown in Fig. 4f, compared with the normal tandem OLED without DSL, all the four tandem OLEDs with DSL show enhanced power efficiency. The maximum power efficiency for the C60-, NPB-, Alq_3- and Bphen-based tandem OLEDs are 2.61, 1.92, 1.74 and 1.71 lm/W respectively, which are much higher than the 1.47 lm/W for the normal tandem OLED without DSL. If we further compared with the maximum power efficiency

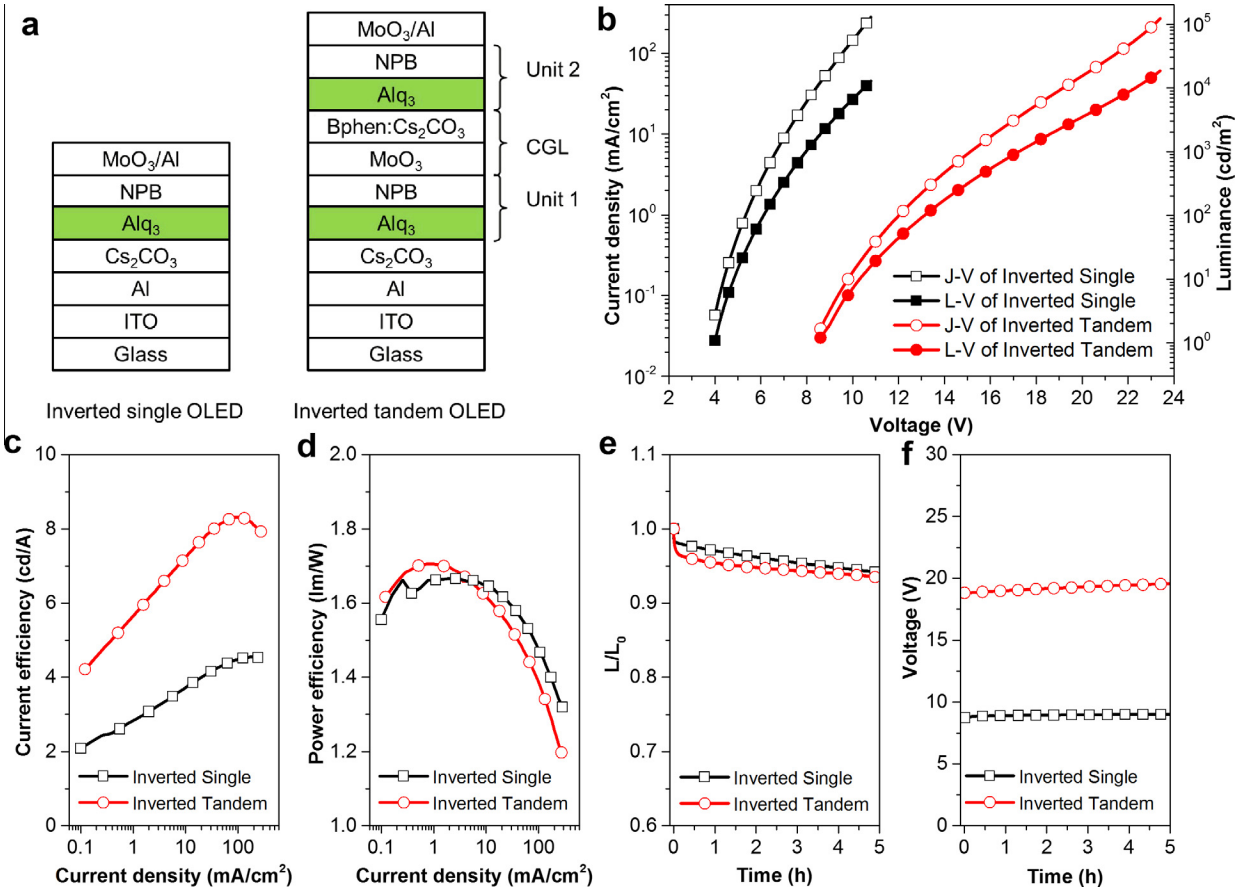

Fig. 2. Device structures and performances of the inverted single and inverted tandem OLEDs. (a) Device structures for the inverted single and inverted tandem OLEDs. The CGL for the inverted tandem OLED is NPB/MoO_3 (10 nm)/Bphen:30 wt.% Cs_2CO_3 (20 nm). (b) *J*–*V* and *L*–*V* curves for the two OLEDs. (c) Current efficiency vs. current density curves and, (d) power efficiency vs. current density curves for the two OLEDs. (e) Luminance and, (f) voltage degradation curves for the two OLEDs.

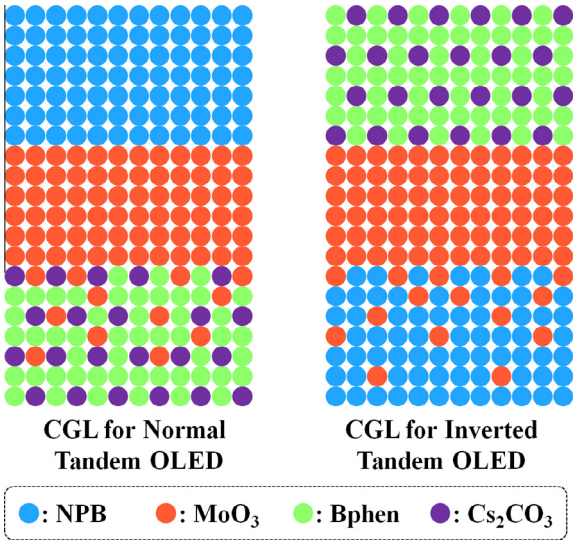

Fig. 3. The charge generation layers in the normal tandem OLED and inverted tandem OLED. In the CGL for the normal tandem OLED, the MoO_3 will diffuse into the underlying Bphen.

(1.69 lm/W) of the normal single OLED, the enhancement ratios for the C60- and NPB-based tandem OLEDs are 54.4% and 13.6%, respectively, which are mainly derived from the significant voltage reductions. Actually, researchers have been searching for such CGLs for a very long time. Compared with existing approaches, our DSL-based CGL have obvious advantages, such as simple structure and large enhancement factors.

Next, we examined the long-term stability of these devices. As shown in Fig. 5a, as expected, all the four tandem OLEDs with DSL show great improvement in term of luminance degradation and the difference between different DSLs is marginal. And there is also obvious improvement for the voltage degradation, as can be seen in Fig. 5b, but there is difference between different DSLs. The voltage increase ratios for different DSLs were shown in Fig. 5c and it follows an order of $\Delta V/V_0(\text{Bphen}) > \Delta V/V_0(\text{Alq}_3) > \Delta V/V_0(\text{NPB}) > \Delta V/V_0(\text{C60})$. To link the voltage degradation to the properties of the DSLs, we plot the $\Delta V/V_0$ against the thermal evaporation temperatures (T_{evap}) and energy levels (HOMOs and LUMOs) of the DSLs. As shown in Fig. 5d, the $\Delta V/V_0$ shows clear dependence on T_{evap}, the higher T_{evap} the smaller the $\Delta V/V_0$, while there is no clear relation between the HOMOs/LUMOs and $\Delta V/V_0$. Actually, the T_{evap} reflects the thermal stability of the DSLs, the one with higher T_{evap} has better resistance to the diffusion of MoO_3 and the result tandem OLED would show better stability. While due to there is no clear relation between the long-term stability and energy levels of DSLs, the energy level alignment in this type CGL seems not that important. At this point, it is very clear that the fast degradation of the normal tandem OLED without the DSL is due to the diffusion of MoO_3 into Bphen:Cs_2CO_3 layer and this diffusion process can be suppressed by inserting a thin DSL. After knowing this, we can then understand the turn-on voltage difference shown in Fig. 4d. Due to the diffusion of MoO_3 happens at the device fabrication process, there is already somewhat

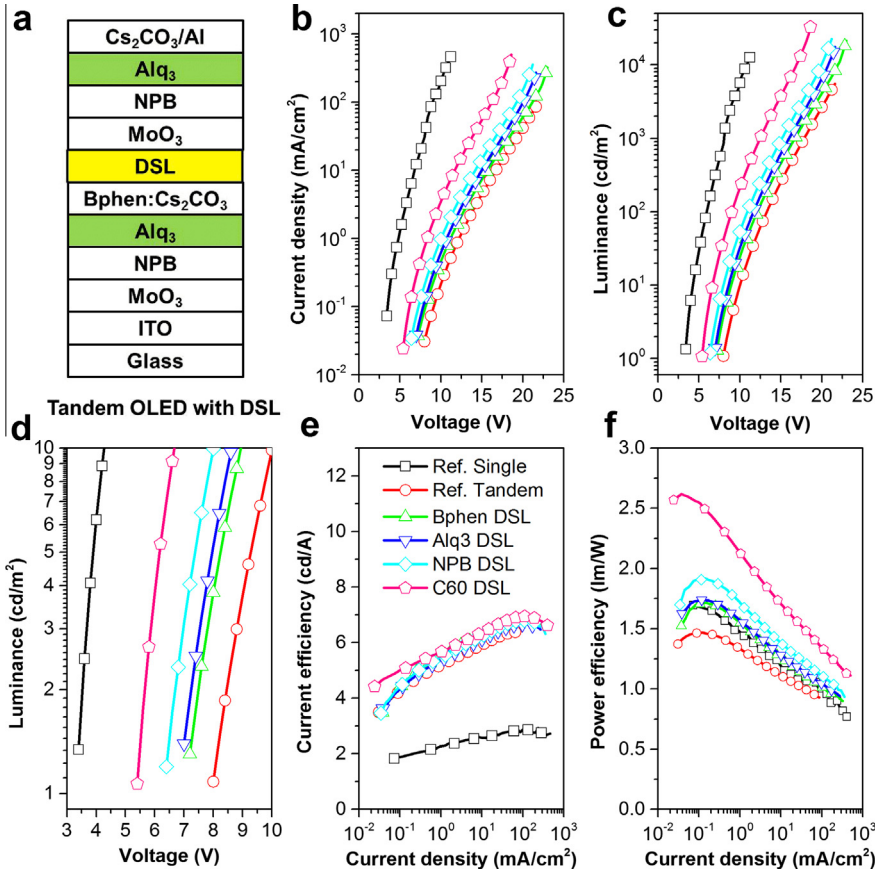

Fig. 4. Structures and performances of normal tandem OLEDs with diffusion suppressing layer. (a) Device structures, (b) *J–V*, (c) *L–V*, (d) *L–V* zoom out, (e) current efficiency vs. current density and, (f) power efficiency vs. current density curves for the normal tandem OLEDs with different DSLs. The thicknesses for all the DSLs are 5 nm. The used DSLs are NPB, Bphen, Alq_3 and C60.

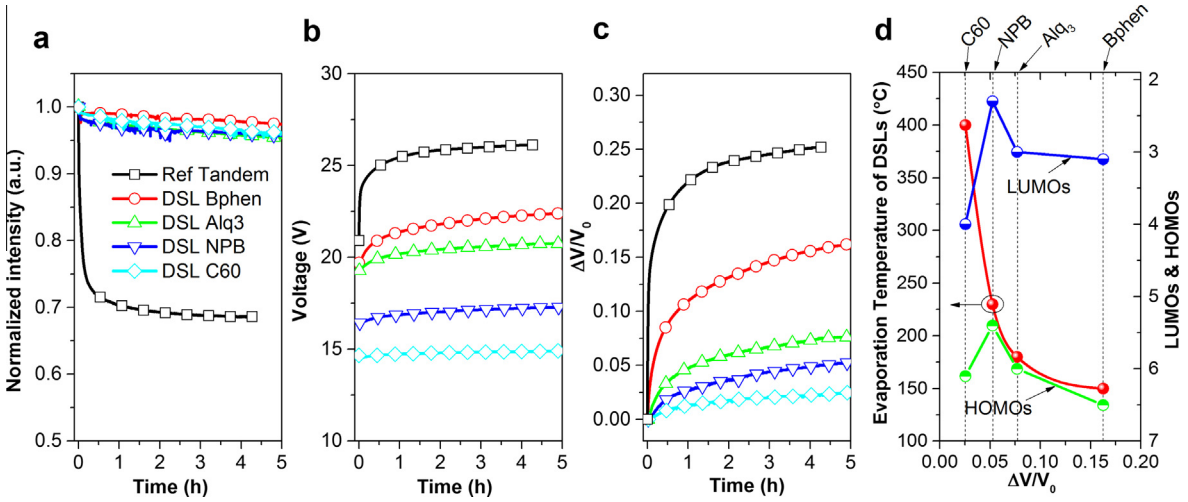

Fig. 5. Degradation comparison of normal tandem OLEDs with DSLs. (a) Luminance, (b) voltage degradation process comparison of tandem OLEDs without and with Bphen, Alq_3, NPB and C60 DSLs. (c) Voltage changing ratio curves for (b). (d) Dependences of voltage changing ratio on energy levels (LUMOs and HOMOs) and evaporation temperatures of the DSLs.

degradation before the measurements were made. Thus the device will have larger turn-on voltage if the corresponding DSL has less resistance to the MoO_3 diffusion.

4. Conclusion

In conclusion, we have looked into the long-term stability issue of TMO based tandem OLED, which was not well addressed before. We found that in the real device, TMO will diffuse into the underlying n-doped ETL. For metal compounds based n-type dopant, such as Cs_2CO_3, this diffusion process will cause severe degradation to the CGL under electrical bias. We proposed and identified that introducing a DSL can suppress the mass diffusion of TMO and the result tandem OLEDs showed very good performance in terms of turn-on voltage, power efficiency and long-term stability. Our finding also indicates that the interfaces in organic optoelectronic

devices sometimes can cause very large difference and should be considered seriously when obvious inter-diffusion happens. Further studies will extend this idea to different n-type dopants and TMOs and it is also important to do the elemental depth profiling of the diffusion process to provide direct evidence for above research.

Acknowledgement

This work is supported by the National Research Foundation of Singapore under Grant No. NRF-CRP-6-2010-2.

Appendix A. Supplementary data

Supplementary data associated with this article can be found, in the online version, at http://dx.doi.org/10.1016/j.orgel.2015.04.010.

References

[1] C.W. Tang, S.A. Vanslyke, Appl. Phys. Lett. 51 (1987) 913.
[2] C. Féry, B. Racine, D. Vaufrey, H. Doyeux, S. Cinà, Appl. Phys. Lett. 87 (2005) 213502.
[3] J. Kido, T. Matsumoto, T. Nakada, J. Endo, K. Mori, N. Kawamura, A. Yokoi, SID Symp. Dig. Tech. Papers 34 (2003) 964.
[4] L.S. Liao, K.P. Klubek, C.W. Tang, Appl. Phys. Lett. 84 (2004) 167.
[5] S.L. Lai, M.Y. Chan, M.K. Fung, C.S. Lee, S.T. Lee, J. Appl. Phys. 101 (2007) 014509.
[6] Y.H. Chen, D.G. Ma, J. Mater. Chem. 22 (2012) 18718.
[7] X. Qi, N. Li, S.R. Forrest, J. Appl. Phys. 107 (2010) 014514.
[8] L.S. Liao, K.P. Klubek, Appl. Phys. Lett. 92 (2008) 223311.
[9] M. Kroeger, S. Hamwi, J. Meyer, T. Riedl, W. Kowalsky, A. Kahn, Appl. Phys. Lett. 95 (2009) 123301.
[10] Q.Y. Bao, J.P. Yang, J.X. Tang, Y.Q. Li, C.S. Lee, S.T. Lee, Org. Electron. 11 (2010) 1578.
[11] S. Hamwi, J. Meyer, M. Kroger, T. Winkler, M. Witte, T. Riedl, A. Kahn, W. Kowalsky, Adv. Funct. Mater. 20 (2010) 1762.
[12] J. Meyer, S. Hamwi, M. Kroger, W. Kowalsky, T. Riedl, A. Kahn, Adv. Mater. 24 (2012) 5408.
[13] D.S. Leem, J.H. Lee, J.J. Kim, J.W. Kang, Appl. Phys. Lett. 93 (2008) 103304.
[14] Y.-H. Deng, Q.-D. Ou, Q.-K. Wang, H.-X. Wei, Y.-Q. Li, S.-T. Lee, J.-X. Tang, J. Mater. Chem. C 2 (2014) 1982.
[15] C.-W. Chen, Y.-J. Lu, C.-C. Wu, E.H.-E. Wu, C.-W. Chu, Y. Yang, Appl. Phys. Lett. 87 (2005) 241121.
[16] C. Diez, T.C.G. Reusch, E. Lang, T. Dobbertin, W. Brütting, J. Appl. Phys. 111 (2012) 103107.
[17] S.-Y. Chen, T.-Y. Chu, J.-F. Chen, C.-Y. Su, C.H. Chen, Appl. Phys. Lett. 89 (2006) 053518.
[18] H. You, Y. Dai, Z. Zhang, D. Ma, J. Appl. Phys. 101 (2007) 026105.
[19] Y. Zhao, J. Zhang, S. Liu, Y. Gao, X. Yang, K.S. Leck, A.P. Abiyasa, Y. Divayana, E. Mutlugun, S.T. Tan, Q. Xiong, H.V. Demir, X.W. Sun, Org. Electron. 15 (2014) 871.